JOURNAL OF PROTEOMICS 75 (2012) 1547–1562

Available online at www.sciencedirect.com

SciVerse ScienceDirect

www.elsevier.com/locate/jprot

Unraveling the human dendritic cell phagosome proteome by organellar enrichment ranking

Sonja I. Buschow[a,1], *Edwin Lasonder*[b,1], *Radek Szklarczyk*[b], *Machteld M. Oud*[a], *I. Jolanda M. de Vries*[a], *Carl G. Figdor*[a,*]

[a]*Department of Tumor Immunology at the Nijmegen Centre for Molecular Life Sciences, Radboud University Nijmegen Medical Centre, Postbox 9101, 6500 HB Nijmegen, The Netherlands*

[b]*CMBI at the Nijmegen Centre for Molecular Life Sciences, Radboud University Nijmegen Medical Centre, Postbox 9101, 6500 HB Nijmegen, The Netherlands*

ARTICLE INFO

Article history:
Received 7 October 2011
Accepted 22 November 2011
Available online 3 December 2011

Keywords:
Dendritic cell
Phagocytosis
Proteomics
Galectin-9
Antigen presentation
Phagosome interaction network

ABSTRACT

Dendritic cells (DC) take up pathogens through phagocytosis and process them into protein and lipid fragments for presentation to T cells. So far, the proteome of the human DC phagosome, a detrimental compartment for antigen processing and presentation as well as for DC activation, remains largely uncharacterized. Here we have analyzed the protein composition of phagosomes from human monocyte-derived DC. For LC–MS/MS analysis we purified phagosomes from DC using latex beads targeted to DC-SIGN, and quantified proteins using a label-free method. We used organellar enrichment ranking (OER) to select proteins with a high potential to be relevant for phagosome function. The method compares phagosome protein abundance with protein abundance in whole DC. Phagosome enrichment indicates specific recruitment to the phagosome rather than co-purification or passive incorporation. Using OER we extracted the most enriched proteins that we further complemented with functionally associated proteins to define a set of 90 phagosomal proteins that included many proteins with established relevance on DC phagosomes as well as high potential novel candidates. We already experimentally confirmed phagosomal recruitment of Galectin-9, which has not been previously associated with phagocytosis, to both bead and pathogen containing phagosomes, suggesting a role for Galectin-9 in DC phagocytosis.

1. Introduction

Dendritic cells (DC) are crucial for the initiation of effective adaptive immune responses against invading pathogens [1]. Via a variety of cell surface receptors such as Fc-receptor, complement receptors and C-type lectins, DCs take up and process ingested pathogens for presentation of derived antigens on Major Histocompatibility Complexes (MHC) to T cells [2,3]. Large pathogens (e.g. bacteria and fungi) and apoptotic, malignant or virus infected cells enter the DC via phagocytosis, a process responsible for the engulfment of particles larger than 0.5 μm. The formed phagosome subsequently orchestrates both the activation of DCs required for effective antigen presentation as well as the processing of antigens derived from the ingested material for loading onto MHC [4,5]. On the DC surface, and also within the DC phagosome, DC recognize conserved molecular patterns on the ingested material using pattern recognition receptors (PRR) including Toll like receptors (TLR) and C-type

* *Corresponding author at:* Department of Tumor Immunology, Nijmegen Centre for Molecular Life Sciences, Radboud University Nijmegen Medical Centre, P.O. Box 9101, 6500 HB Nijmegen, The Netherlands.
E-mail address: c.figdor@ncmls.ru.nl (C.G. Figdor).
[1] Both authors contributed equally to this work.

1874-3919
doi:10.1016/j.jprot.2011.11.024

lectins (CLR). Upon ligation these receptors initiate downstream signaling cascades leading to altered gene transcription (e.g. DC activation/maturation). Simultaneously, cytosolic proteins and organelles are recruited to the nascent phagosomes to regulate antigen processing and presentation [5]. Thus, the DC phagosome is a detrimental compartment for the initiation of immune responses against a plethora of pathogens as well as against malignant growths. DCs are currently exploited in anti-cancer vaccination and unraveling the precise protein composition of DC phagosomes will greatly improve our understanding of DC phagosomal antigen processing and presentation that ultimately could help us to improve the efficacy of DC vaccines.

Thus far, most proteomics studies on phagosomes were restricted to those of other professional phagocytes, such as macrophages and neutrophils [6–8]. These studies mainly used isolated latex bead containing (LBC) phagosomes and have identified hundreds of postulated phagosomal proteins. Macrophages and neutrophils however are functionally distinct from DCs, focusing on pathogen scavenging and destruction rather than antigen presentation [2].

Here we present the first analysis of the proteome of LBC phagosomes from human monocyte derived DC that covers over 300 proteins which we quantified label free by peptide counting according to the emPAI method [9].

Although stringent purification methods result in phagosomal preparations that are highly enriched for phagosomes, they are never 100% pure. With the increased sensitivity of MS even trace amounts of contaminants will be picked up and thus not all identified proteins will be necessary for the organelle function [6,10,11]. In addition, fusion of phagosomes with lysosomes and/or autophagosomes may lead to the phagosomal incorporation of proteins from organelles that are destined for degradation such as mitochondria or cytosolic components that are damaged or no longer needed.

To select proteins indispensible for phagosome function we used a subtractive proteomics approach [11–14] comparing phagosomal protein abundance to total cellular abundance. This method is based on the notion that enriched proteins are specifically recruited to the phagosome and thus more relevant to the core functions of the organelle. Using this approach which we designate as “organellar enrichment ranking” (OER) and that we have combined with functional association analysis, we specifically removed those proteins that were co-purified or passively incorporated. We extracted a subset of 90 phagosomal proteins that can now be used to more effectively identify novel players on (DC) phagosomes. We have further confirmed the widespread recruitment of the novel phagosomal protein Galectin-9 to both bead and pathogen-containing DC phagosomes.

2. Materials and methods

2.1. Cells

Dendritic cells were *ex vivo* generated from isolated monocytes as described previously [15]. For large scale proteomics analysis of phagosomes, peripheral blood mononuclear cells were isolated from the blood of a healthy donor (with informed consent) by leukaphereses using the Elutra-cell separator (Gambro BCT, Inc.). For smaller scale experiments, monocytes were isolated from buffy coats of healthy donors (with informed consent) using ficoll density gradients followed by plate adherence. For differentiation of monocytes to dendritic cells, cells were cultured for 6 days in XVIVO medium (Lonza) containing 2% human serum supplemented with IL-4 (300 U/ml) and GM-CSF (450 U/ml), both from CellGenix, Germany.

2.2. Phagosome isolation

Phagosomes from DCs were prepared according to previously described methods [16]. In brief, cells were detached using ice cold PBS and were pulsed in suspension with 1 μm antibody-coated streptavidin beads (for preparation of beads see below) for 1 h at 37 °C in XVIVO medium (Lonza) without serum, at a bead to cell ratio of 10:1. Subsequently, cells were washed 3 times to remove unbound beads and chased for an additional hour at 37 °C in XVIVO + 1% human serum. Phagosome maturation was stopped by addition of a large volume of ice-cold PBS. Cells were washed in homogenization buffer (6% Sucrose, 3 mM Imidazole, 50 mM Mg_2Cl, 10 mM N-Ethylmaleimide (NEM), 2 mM Mg_2ATP (Sigma), 1 mM dithiothreitol (DTT; Sigma), pH 7.4) including inhibitor cocktails of proteases (Complete, Roche) and phosphates (Phosphostop Roche). After washing cells were re-suspended in homogenization buffer with protease inhibitors and were broken by passage through a 2 ml Syringe with a 21 g needle. The homogenization was carried out until 90% of cells were broken without major damage of the nucleus, which was monitored by light microscopy. Nuclei and intact cells were removed following centrifugation at $200 \times g$ for 5 min at 4 °C (without brake) and the post-nuclear supernatant was adjusted to 40–45% sucrose, placed on a cushion of 65% sucrose and layered with a sucrose gradient composed of 35, 25and 10% in 3 mM imidazole pH 7.4. Samples were centrifuged at $100{,}000 \times g_{max}$ for 1 h (4 °C) and enriched phagosome fractions were collected from the 10% and 25% interface of the sucrose gradient. For flow cytometry studies, phagosomes were further treated as described in the flow cytometry analysis section below. For proteomic analysis or Western blotting phagosome fractions were pelleted in ice cold PBS by centrifugation for 30 min at $40{,}000 \times g_{max,}$ dissolved in Laemmli sample buffer and stored at −20 °C until further use.

2.3. Western blotting

Proteins were separated by SDS-PAGE on pre-casted SDS gradient gels (4–20%, Pierce), transferred to Immobilon-P membranes (Millipore, Bedford, MA) and immunolabeled according to standard Western blotting procedures. After labeling, Western blots were scanned by the Odyssey imager (LI-COR Biosciences).

2.4. Flow cytometry analysis of purified phagosomes

Floated phagosomes were fixed in 1% paraformaldehyde (PFA), 0.1 M phosphate buffer pH 7.4 for 15 min on ice. Fixation

was quenched by the addition of an equal volume of 1 M glycine in PBS. Fixed phagosomes were collected by centrifugation at full speed (14,000 rpm) in an Eppendorf centrifuge and permeabilized and immunolabeled in PBS with 1% BSA, 0.1% Saponin (Riedel-de Haën) at room temperature. Prior to antibody labeling, nonspecific binding was blocked using normal sera of secondary antibodies.

2.5. Confocal microscopy analysis

For confocal microscopy analysis, day 6 monocyte derived DCs were attached for 1 h to fibronectin-coated glass coverslips in medium without added serum. Beads (cell to bead ratio 1:10), or FITC-labeled zymosan (1:5), FITC-labeled heat killed *Candida albicans* (1:5) or FITC-labeled heat killed *S. aureus* (1:5) were centrifuged onto the cells in a plate spinner (Hettich) at 500×*g* for 5 min at and incubated at 37 °C for indicated times. Cells were fixed in 4% PFA in 0.1 M phosphate buffer pH 7.4, and subsequently were permeabilized and immunolabeled in PBS with 1% BSA, 0.1% Saponin. Prior to antibody labeling non-specific binding was blocked using normal sera of the species of origin of applied secondary antibodies. For co-capping experiments day 6 monocyte derived DCs were incubated with primary antibodies for 30 min on ice after which cells were thoroughly washed and capping was allowed by incubating the cells with secondary antibodies for 60 min at 15 °C. Subsequently cells were washed and fixed, mounted on poly-L-lysine coated coverslips and analyzed by confocal microscopy using. Cells were analyzed by Olympus FV1000 Confocal Laser Scanning Microscope. The Pearson correlation coefficient was calculated by applying the Image J (http://rsb.info.nih.gov/ij/,) plug-in JACoP [17].

2.6. Antibodies

Bead preparation: We used a multi-step procedure to coat the beads with the anti-DC-SIGN antibody and to ensure the correct orientation of the antibodies (DC-SIGN binding part directed outwards). YG 1 μm streptavidin beads (Polysciences) were first coated with biotinylated Fab_2 rabbit anti-human (Jackson ImmnunoResearch, UK) antibodies. Fab_2 coated beads were then allowed to bind the humanized form (i.e. containing a human Fc-region) of the murine anti-DC-SIGN antibody (AZN D1, produced by Alexion Pharmaceuticals and described in [18]).

The following primary antibodies were used for Western blotting and confocal analysis: mouse anti-human HLA DR/DP/DQ (clone CR3/43; Dako), Rabbit anti-human DC-SIGN (H200, Santa Cruz), Mouse anti-human LAMP1 (clone H4A3, Biolegend), Rabbit anti-LAMP 1 (clone L1418, Sigma), mouse anti-human CD44 (clone G44-26, BD biosciences), mouse anti-human Cathepsin D (clone 49, BD biosciences), Goat anti-human Galectin-9 (R&D systems), mouse anti-rat PDI (Affinity Bioreagents), mouse anti-Actin (clone AC-40, Sigma), Goat anti-Moesin (C15, Santa Cruz Biotechnology), Rabbit anti-Cofilin (Cell Signaling). IRDye conjugated secondary antibodies for Western blotting were obtained from LI-COR Biosciences, and Alexa-647 conjugated secondary antibodies for flow cytometry and confocal analysis were from Invitrogen.

2.7. Sample preparation for LC–MS/MS experiments

Samples from two batches of purified phagosome preparations (20×10^6 phagosomes per batch) were incubated for 5 min at 95 °C in Laemmli sample buffer containing β-mercaptoethanol (Sigma) prior to loading onto a 4–20% gradient TRIS/Bis Ready Gel (Biorad). After electrophoreses, protein gels were stained using the Novex colloidal blue staining kit (Invitrogen) and divided into several slices. Proteins of batch 1 were divided into 6 slices per gel lane and proteins of batch 2 were concentrated into a single slice by a short electrophoresis running time of approximately 15 min. Gel slices were treated with DTT and iodoacetamide and digested by trypsin [19]. Digested samples were acidified to a final concentration of 0.1% TFA and purified by STAGE tips [20].

2.8. Liquid chromatography tandem mass spectrometry

Peptide sequencing experiments were performed by LC–MS/MS using a nano HPLC Agilent 1100 LC system connected to a 7-Tesla linear ion trap ion cyclotron resonance Fourier transform (LTQ-FT Ultra) mass spectrometer (Thermo Fisher, Bremen, Germany). Peptides were separated on 15 cm 100 μm ID PicoTip columns (New Objective, Woburn, USA) packed with 3 μm Reprosil C18 beads (Dr. Maisch GmbH, Ammerbuch, Germany) using a 120 and a 240 min gradient from 12% buffer B to 40% buffer B (buffer B contains 80% acetonitrile in 0.5% acetic acid) with a flow-rate of 300 nl/min for digests from batch1 and batch 2 respectively. Peptides eluting from the column tip were electrosprayed directly into the mass spectrometer with a spray voltage of 2.2 kV. Data acquisition with the LTQ-FT instrument was performed in a data-dependent mode to automatically switch between MS and MS2. Full-scan MS spectra of intact peptides (m/z 350–1500) with an automated gain control accumulation target value of 1,000,0000 ions were acquired in the Fourier transform ion cyclotron resonance cell with a resolution of 50,000. The four most abundant ions were sequentially isolated and fragmented in the linear ion trap by applying collisionally induced dissociation using an accumulation target value of 10,000, a capillary temperature of 100 °C, and a normalized collision energy of 27%. A dynamic exclusion of ions previously sequenced within 180 s was applied. All unassigned charge states and singly charges ions were excluded from sequencing. A minimum of 200 counts was required for MS2 selection. Maximum injection times were set at 500 ms and 400 ms respectively for FT MS and IT MS/MS measurements.

2.9. Peptide identification by MASCOT

Raw spectrum files were converted into Mascot generic peak lists by MaxQuant version 1.0.13.13 (http://maxquant.org/) using the default setting to extract the top 6 MS MS peaks per 100 Da [21]. Proteins were identified by searching peak lists containing fragmentation spectra with Mascot version 2.2 (Matrix Science) against the human International Protein Index (IPI) database version 3.56 (ftp://ftp.ebi.ac.uk/pub/databases/IPI/) supplemented with frequently observed contaminants and concatenated with reversed copies of all entries. Mascot search parameters for protein identification specified a mass tolerance of 10 ppm for the parental peptide

and 0.5 Da for fragmentation spectra and a trypsin specificity allowing up to 3 miscleaved sites. Carbamidomethylation of cysteines was specified as a fixed modification, and oxidation of methionine, deamidation of glutamine and asparagine were set as variable modifications. The required minimal peptide length was set at 6 amino acids. Internal mass calibration of measured ions and peptide validation by establishing false discovery rates (FDR) was performed by MaxQuant as described [21]. We accepted peptides (charge state >1, nr variable modifications <4) and proteins (nr unique peptides >1) with a FDR better than l%. Assembling of peptide sequences on protein groups was performed by maximum parsimony in MaxQUANT.

Proteomics data was deposited at HumanProteinPedia (www.humanproteinpedia.org), accession numbers HuPA00683 (all proteins) and HuPA00684 (extended OER derived protein set) and these peptide and protein lists are provided as supplementary data (Supplementary Tables 1 and 2).

2.10. Protein quantification by protein abundance index

The exponentially modified protein abundance index emPAI method [9,22] was used to quantify the proteins by a label free approach based on peptide counting, where emPAI values are calculated according to Eq. (1):

$$emPAI = 10^{PAI} - 1 \text{ with } PAI = n_{\text{observed peptides}}/n_{\text{observable peptides}}. \quad (1)$$

The number of 'observable' peptides per protein was calculated for peptides in the mono isotopic mass range of 698–4000 from the output of the program Protein Digestion Simulator (http://ncrr.pnl.gov/software/), which computes peptide masses and hydrophobicities of simulated digests of protein databases in FASTA format. Protein emPAI values were calculated from peptide identifications of merged LC–MS/MS runs per phagosome sample (Supplementary Table 2). The emPAI expression data of two phagosome samples was averaged after normalization. Normalization between phagosome and immature DC proteomes (see next section) was performed based on median emPAI abundance values.

2.11. Immature DC proteome

The human immature DC proteome was determined by us in a previous study [23], where peptides were mapped to the human IPI database version 3.25 and proteins were quantified by the emPAI method. In order to compare the newly generated data with the immature DC proteome, peptides of both datasets were mapped to the proteins of the human IPI database version 3.56 using the software package Protein Coverage Summarizer (http://ncrr.pnl.gov/software/).

2.12. Assembling of phagosome proteome by organellar enrichment ranking

Enrichment ranking of proteins detected in the phagosome preparations and in immature DCs was performed by sorting proteins on enrichment factors, which are calculated according to Eq. (2):

$$Enrichment\,factor = norm.\,emPAI\,phagosome\,prep/norm.\,emPAI\,immature\,DCs. \quad (2)$$

A total of 6 proteins (FN1, SLC37A2, P2RX4, SCAMP3, HTATIP2) were uniquely present in the phagosome dataset and not detected in immature DC. These proteins could either be highly enriched, differentially expressed in DCs and phagosome donor or finally serum derived; a distinction we cannot make based on the available data and therefore we do not study these proteins any further here.

The enrichment ranked protein list was evaluated initially by the distribution of manually-curated positive and negative marker sets (for positive and negative markers see Supplementary Table 2). We determined the enrichment factor threshold at the most optimal balance between false positives and false negatives at the enrichment factor t that leads to the highest F_1 score (a well-established accuracy test; Eq. (3)):

$$F_1 = 2 * precision * recall/(precision + recall) \quad (3)$$

where $precision = Pm^{\geq t}/(Pm^{\geq t} + Nm^{\geq t})$

and $recall = Pm^{\geq t}/(Pm^{\geq t} + Pm^{<t})$

where Pm denotes the positive marker set and $Pm^{>t}$ denotes the number of proteins from the positive marker set that exceeds (≥t) or falls below (<t) the cut-off enrichment threshold. Analogously, Nm denotes the negative marker set.

The quality of the final phagosome proteome was determined by estimation of recall value (fraction of recovered proteins of the positive marker set, defined above) and the corrected False Discovery Rate (cFDR, to account for the fraction of proteins incorrectly assigned to phagosome). cFDR was calculated over all detected proteins, corrected for the phagosomal proteome size according to Eq. (4):

$$cFDR = cFP/(cFP + cTP). \quad (4)$$

The cFP (false positive; Eq. (5)) and cTP (true positive; Eq. (6)) are proteome-wide corrected fractions that account for the discrepancy between the size of the maker sets and the size of phagosome. The proteome-wide correction takes into account the prior knowledge about the fraction of proteome that localizes to the phagosome ($P_{\text{phagosome}}$)

$$cFP = (1\text{–}specificity) * (1\text{–}P_{\text{phagosome}}) \quad (5)$$

where $\text{specificity} = \dfrac{Nm^{<t}}{Nm^{<t} + Nm^{\geq t}}$

$$cTP = recall * P_{\text{phagosome}} \quad (6)$$

where cFP and cTP are derived from positive and negative marker sets, accounted for the phagosomal proteome size.

2.13. Gene ontology analysis

Gene ontology analysis was performed using the internet based tool DAVID of the national institute of Allergy and Infectious Disease (http://david.abcc.ncifcrf.gov/home.jsp) [24,25]. P-values for significant pathway enrichment of phagosomal proteins as compared to a background of proteins identified in whole immature DC was calculated using a modified fisher exact test (EASE) to which a Bonferroni correction for multiple testing was applied.

2.14. *Comparison DC phagosome proteome with published phagosome proteomes of human and mouse antigen presenting cells*

The proteomic data mining software package ProteinCenter (Proxeon Bioinformatics, Odense, Denmark) was used to compare our data with previous phagosome proteome data derived from three human cell lines [26,27] and from one mouse cell line [28] (Supplementary Table 3). Human orthologs of mouse genes were taken from the Human & Mouse Orthologous Gene Nomenclature (HUMOT) database (http://www.genenames.org/activities/humot/). In ProteinCenter, these datasets were imported and clustered based on a sequence similarity of 95% with the optimization option "most homogeneous groups". This ensures that protein redundancy between the different datasets is absent, and allows for finding DC specific phagosomal proteins.

2.15. *Functional interaction network*

Protein functional interactions for the network were downloaded from String 8.3 (http://string-db.org/) and analyzed with custom Python scripts [29]. For the rescuing proteins using the functional association data, multiple network thresholds of the combined score (0.5, 0.7., 0.9) and topology constraints (2–4 neighboring nodes from the enriched dataset) were tested to choose the final parameters. The final parameters (0.5 and 4 respectively) do not introduce proteins from the negative dataset (see Supplementary Table 4).

3. Results

3.1. *Phagosome isolation and characterization*

So far, most phagosome proteomic analyses were performed with macrophage like cell-lines that are easily cultured into the large amount needed for phagosome isolation and detection by mass spectrometry (MS). Here we set out to determine for the first time the protein composition of phagosomes from a primary culture of human monocyte-derived DCs. These DC do not divide and can therefore only be obtained in limited amounts. Bare latex beads are not efficiently taken up by DCs (data not shown). To obtain sufficient phagosomes from these cells for MS analysis we promoted bead uptake by using beads that were antibody targeted to the DC-specific C-type lectin receptor DC-SIGN that is highly expressed by DCs and involved in the recognition and uptake of many different pathogens [30,31]. The antibody used for this purpose (AZN-D1) does not induce DC-SIGN signaling and has a modified Fc region that cannot be recognized by the Fc-receptors expressed on DC [18,32]. These beads thus allow us to specifically exploit only the uptake properties of DC-SIGN without influencing the phagosome by DC-SIGN signaling. During a 1 h pulse, DC-SIGN targeted latex beads were readily taken up by 60–80% of the cells with an average of 6–8 beads per cell (Supplementary Fig. 1). After a subsequent 1 h chase we isolated LBC containing phagosomes using well established sucrose gradient floatation [16]. For MS analysis, we isolated phagosomes in duplicate from DCs generated from two separate leukaphereses events of one healthy donor. We checked isolated phagosomes by contrast microscopy in combination with fluorescent labeling. Microscopy analysis demonstrated that the phago-lysosomal marker protein LAMP1 was surrounding the purified latex bead containing compartments and showed also that the isolate was free of other large compartments or associated/co-purified membranes (Supplementary Fig. 2).

Using MS analysis we found 328 proteins to be present in both phagosomal preparations with a minimum of two unique peptides per preparation (Supplementary Table 1).

Additional information on sample purity was obtained from the MS identified proteins themselves; we performed a Gene Ontology (GO) enrichment analysis for the root term "cellular component". To prevent false overrepresentation of terms associated to DC function, we used as a reference set the proteome of whole immature DCs that we have described recently [23]. Many GO terms describing components associated to phagosome formation including vesicle, vacuole, lysosome and plasma membrane (Fig. 1) were significantly overrepresented in the phagosome proteome compared to the reference set, confirming that our preparation was indeed highly enriched for phagosomes.

Recently, there has been much debate on the involvement of ER in DC phagocytosis to explain crosspresentation of exogenous phagocytosed antigens on MHC I. ER was, as a cellular component, not found to be significantly overrepresented in our GO analysis, similar to mitochondrial or peroxisomal proteins (Fig. 1 and Supplementary Fig. 3). Moreover, in contrast to GO ER annotated proteins that were not detected in phagosomes, most phagosomal identified ER protein were also annotated to other GO terms indicating they may even have had an origin other than ER (data not shown).

In addition, we inspected ER derived components of the MHC I loading machinery and found that 5 (Calnexin, Calreticulin, PDI-A3, HSPA5, HSPA1) out of the 8 proteins (62%) belonging to the machinery and detected in DC were also identified on phagosomes (but not TAP1, TAP2 and Tapasin).

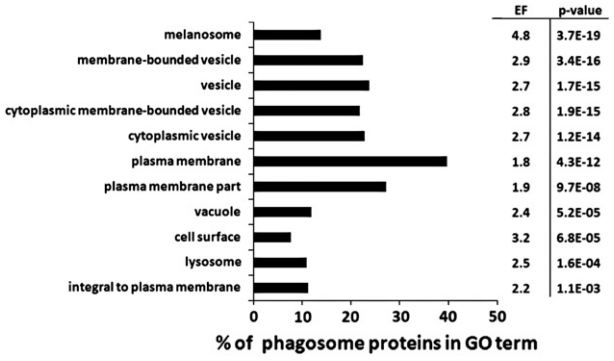

Fig. 1 – Gene Ontology analysis of phagosomal proteins. Shown are GO terms significantly overrepresented in the phagosome dataset with respect to the dataset containing all proteins detected in immature DCs. Horizontal bars display the percentage of phagosome proteins that annotated to each GO term and columns lists their enrichment factor (EF) over whole DC and the EASE derived p-value for overrepresentation (corrected for multiple testing).

Their overrepresentation on phagosomes may indicate specific recruitment to the phagosome relative to other proteins annotated to GO ER of which only 15% was found back on phagosomes (44 out of 266).

We then compared proteins identified from our DC phagosomes to the available human phagosome proteomes, isolated from neutrophils [26] (198 proteins) and THP-1 cells [27] (288 proteins in LBC) and to the recently published most elaborate analysis of murine RAW macrophages phagosomes [28] (2415 proteins) and found an overlap of 51, 139, and 233 proteins respectively (Supplementary Table 3). Notably, over 70 proteins were not previously identified in these three datasets and may thus be DC-specific. Consistent with the specific function of DC in antigen presentation among these DC specific phagosomal proteins were several HLA and CD1 molecules that present protein and lipid antigens, as well as the pattern recognition receptors DC-SIGN and TLR8 that modulate and trigger DC maturation respectively [33,34]. Shared with other phagocytes were other transmembrane receptors involved in particle uptake and recognition including Mac-1, CD14 and CD44 (Supplementary Table 3). Also established phagosomal proteins important for lysosome function, trafficking and biogenesis such as LAMP 1 and 2, the V-ATPase complex and many Rab GTPases were readily identified in DC phagosomes.

For all identified proteins in each preparation we also obtained a measure for their abundance using a label free peptide counting method designated emPAI (exponentially modified Protein Abundance Index; Supplementary Table 2) developed by Ishihama et al [9]. This allowed us to rank proteins according to their abundance. We first used the quantitative information to look in more detail at established phagosomal proteins reflecting phagosomal age (Table 1). Ranking on abundance confirmed the lysosomal state of the phagosomes, that is expected after a 1 h pulse followed by a 1 h chase. Lysosomal constituents LAMP1 and the components of the V-ATPase complex are highly abundant as is the late endosomal marker Rab7 that is more prominent than markers of earlier endosomes such as Rab5 and Rab11. Furthermore HLA II dominates over HLA I consistent with their preferential association to late and early endosomes respectively (Supplementary Fig. 3).

Despite our stringent purification procedure and similar to previous reported latex bead phagosomes proteomes [6], we also identified several proteins that are not likely to be functionally relevant for phagosome (e.g. histones, ribosomal proteins) but that may have become passively associated to the isolated phagosome by autophagy or aspecific adherence. Thus, even though the GO analysis demonstrated that our preparation was highly enriched in phagosomal proteins, not all of the proteins identified are necessary for the core functions of the phagosome. The presence of these co-purified proteins severely hampers the selection of potentially novel phagosomal proteins from our dataset. Therefore an additional filtering step is required to distinguish such proteins.

3.2. *Defining the phagosome proteome by organellar enrichment ranking*

To be able to more effectively select (novel) phagosomal proteins important for organelle function, we developed a subtractive proteomics approach based on protein abundance in the phagosome preparation relative to immature DCs, the cells from which they originate. Although most proteins relevant for phagosomes will not be exclusively present on phagosomes, we expect that many phagosomal proteins important at this stage of phagocytosis will be specifically recruited to the phagosome and may thus be more abundant in phagosomes as compared to the rest of the cell. Ideally these proteins would show an enrichment factor greater than 1. We determined protein enrichment ratios by dividing the average emPAI values of proteins in phagosomes by the emPAI values obtained in immature DCs (Supplementary Table 2). Even though datasets were normalized in advance (see Materials and methods), it should be noted that the enrichment factor thus obtained is only an estimate because phagosome and immature DC data were analyzed separately and were also obtained from different donors. Nevertheless, most proteins, except for 6 (see Materials and methods), in the phagosome dataset were also present in the immature DC dataset and could thus be used for comparison (Supplementary Table 2). Of the remaining set of 322 proteins, we sorted phagosomal proteins on relative enrichment ratios compared to whole DC, a method we here designate as "organellar enrichment ranking" or OER. By OER we expect to find many phagosomal proteins important for the organelle at this stage among the most enriched proteins (top of the list), and proteins most likely co-purified (e.g. histones) amongst the most depleted proteins (bottom of the list). To further evaluate the ranked list, golden standard sets of phagosomal proteins and co-purified proteins, are needed. We composed a positive marker list by manual curation of identified proteins that are beyond any doubt, based on non-MS experiments, associated to the DC phagosome at this time-point, including HLA proteins, the vacuolar ATPase complex, the NADPH oxidase components (Nox2) LAMP proteins and Cathepsin proteases (a total of 20 proteins indicated in Supplementary Table 2) [2,35]. Indeed, proteins of this positive marker set are more abundant on phagosomes and also more enriched (Fig. 2). In addition, we manually composed a set of negative markers (e.g. proteins most likely passively co-purified with no specific function in phagosome biogenesis) that includes proteins annotated to GO terms describing ribosomes, mitochondria and nucleus (a total of 45 proteins indicated in Supplementary Table 2). Negative markers were not necessarily less abundant than positive markers, demonstrated by random distribution over the abundance ranked list (Fig. 2). Negative markers were however, much less enriched and thus depleted from the top end of the enrichment ranked list (Fig. 2). This demonstrates that OER is an efficient method to select proteins with established functional relevance for the DC phagosome at this stage and to deplete for proteins that do not likely actively contribute.

We used a statistical approach to determine the optimal enrichment factor threshold; the F1 score. The F1 score takes into account the distribution of both positive and negative marker sets (mean between recall and precision, see Materials and methods). We calculated the sensitivity and the specificity (within the boundaries of our dataset and marker sets) as well as an F1 score for each enrichment factor (emPAI ratio value; Fig. 3). A maximal F1-score (0.77) was achieved at an enrichment factor of 0.75 where 70% of positive

Table 1 – Abundance of proteins frequently associated to phagocytosis. Listed are proteins classified by functional groups which are frequently associated to phagocytosis. Protein abundance is shown as the average emPAI value for two phagosome preparations.

Functional group	Gene symbol	Protein abundance
Antigen presentation	HLA-DRA	6.36
	HLA-DRB	4.57
	HLA-DPB1	2.21
	HLA-DMB	1.82
	CD1B	1.18
	HLA-A	0.78
Cell surface receptor	CD209	4.45
	CD44	4.01
	ITGB2	2.70
	ITGAM	2.51
	ITGAX	1.55
	CD14	1.51
	MRC1	1.37
	TFRC	1.12
	ITGB1	0.57
	ICAM1	0.55
	SIRPA	0.39
	ITGA5	0.34
	TLR8	0.24
	LRP1	0.08
Lysosmal enzyme activity	CTSD	14.47
	TPP1	3.60
	ANPEP	3.06
	CTSS	1.92
	ASAH1	1.76
	CSTB	1.69
	ACP2	1.28
	HEXB	1.08
	CTSC	0.90
	ACP5	0.68
	CTSZ	0.62
	GLB1	0.59
	GLB1	0.59
	GNS	0.57
	CAT	0.44
	HEXA	0.37
	FUCA1	0.34
	MAN2B1	0.31
	GANAB	0.22
	GAA	0.22
	GBA	0.21
Endosome/lysosome	LAMP1	1.72
	CYBB	1.62
	M6PR	0.70
	NPC1	0.64
	LAMP2	0.57
V-ATPase	ATP6V1A	9.41
	ATP6V1B2	8.39
	ATP6V0D1	4.36
	ATP6V1E1	3.86
	TCIRG1	2.13
	ATP6V1H	1.68
	ATP6V0A1	1.47
	ATP6V1C1	1.40
	ATP6V1D	1.16
Rab proteins	RAB7A	17.99
	RAB5C	8.53
	RAB1A	4.34
	RAB11B	2.90
	RAP2B	2.86
	RAB14	2.82
	RAB8A	2.27
	RAB2A	2.21
	RAB21	1.60
	RAB18	1.50
	RAB5A	1.04
	RAB32	1.03
	RAB35	1.02
	RAB9A	0.57
SNAREs	STX7	2.39
	NAPA	2.38
	STX12	2.20
	VAMP7	1.69
	STX8	0.91
	SEC22B	0.84
	NSF	0.79
	STXBP2	0.76

markers were included (sensitivity) and 96% of negative markers were excluded (specificity). This threshold yields an OER-derived subset of 73 phagosomal proteins.

For this set we calculated the corrected False Discovery Rate (cFDR, see Materials and methods) that takes into account the maximal number of co-purified proteins we expected in the enriched phagosome. With the conservative prior estimation of the number of phagosomal relevant for phagosomal function (100 phagosomal proteins out of 322) we derive a cFDR of 12% (9 out of 73 proteins, see Materials and methods). This is an upper limit on the number of co-purified proteins, and cFDR drops to 7% with the assumption of a larger relevant phagosomal

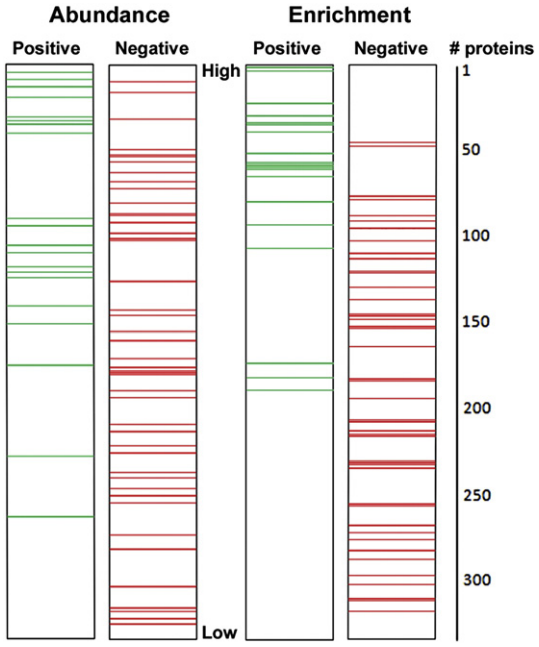

Fig. 2 – Distribution markers upon quantitative sorting. Shown is the distribution of positive and negative marker proteins sorted from highest (top) to lowest (bottom) phagosomal emPAI values (abundance) at the left side and the emPAI enrichment factors at the right side of the figure.

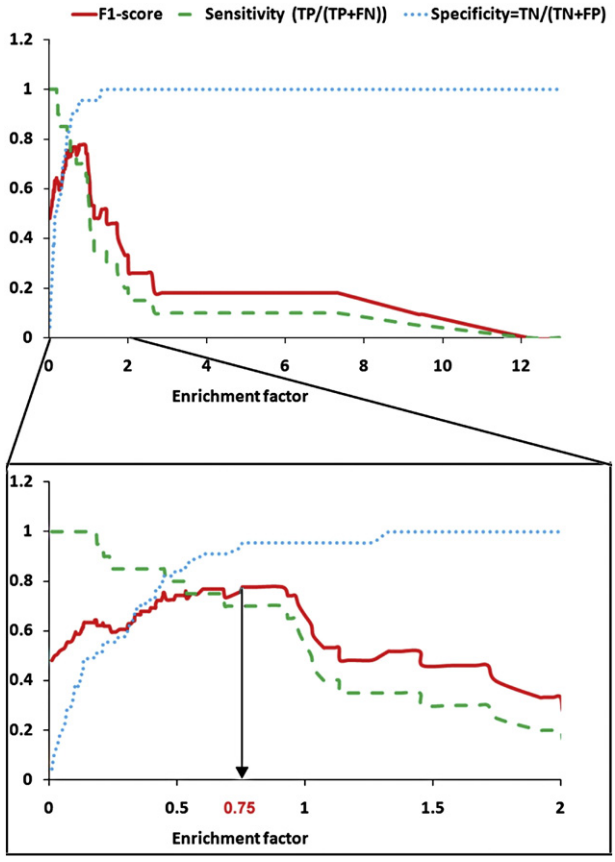

Fig. 3 – Determining the most optimal enrichment factor cut-off using the F1-score. The performance of specificity, sensitivity and F1 score is shown for all enrichment factor thresholds, from low stringency at the left side to high stringency at the right of the figure. The performance parameters were derived from the positive and negative marker sets. The best balance between specificity and sensitivity is found for a stringency (enrichment factor cutoff) that shows the highest F1 score, at an enrichment factor threshold of 0.75.

proteome size of 150 proteins. Prior to the OER analysis, the estimated cFDR, for the same assumptions of 100 phagosomal constituents responsible for its core functions, is 69%. The OER-derived subset of 73 is thus considerably depleted of co-purified proteins (6-fold).

To assess the variability between the two phagosome preparations obtained from different donors we also performed the OER analysis using the single donor EmPAI values and enrichment factors (Supplementary Tables 2 and 5). The single donor derived enriched protein sets were similar to the one obtained using the average of the two donors (overlapping 75% and 88% with the average derived set) but were less effective in removing negative markers (cFDR(100) of 24% and 20% respectively), demonstrating the reproducibility of our data and also the added value of combining the data of two donors. As an alternative approach we also calculated the overlap between sets generated using the individual EmPAI values. This approach proved as efficient in removing negative markers as the average EmPAI values (cFDR(100) of 12%) and even slightly better at retaining positive markers (75%) but at the expense of a lower set size (61 vs 73 proteins). Therefore, we have chosen the average based OER-derived subsets for further investigation.

Next, we evaluated the performance of the OER method by taking a closer look at the nature and interaction between of the components present in the OER-derived proteome. We expect phagosome-related proteins to be further enriched by our method and that the components have a closer interaction than non-phagosomal proteins. First, we performed a GO enrichment analysis of the OER-extracted subset and compared this to the original dataset of 322 proteins (Fig. 4). As anticipated, within the OER-derived proteome (73 proteins), GO terms capturing phagosome-related terms (e.g. vacuole, lysosome), are even further enriched as compared to the initial proteome of 322 proteins (Fig. 4). Again, we also inspected the presence of ER components in the OER subset and did not find them further enriched as compared to the initial set of phagosomal proteins (Supplementary Fig. 3). Interestingly, components of the ER derived MHC I loading machinery as well as the MHC I protein HLA-A were all excluded from the OER subset. In contrast, most MHC II related components were included, suggesting that the phagosome at this time point may focus more on MHC II than on MHC I presentation. Indeed, flow cytometry of isolated DC phagosomes already showed that MHC I is more abundant in earlier phases of phagocytosis suggesting that exclusion of MHC I and its loading machinery from the OER subset may be a result of their diminished presence on later phagosomes (Supplementary Fig. 4).

Next, the functional association between the phagosome proteome components was analyzed using the network of functional protein interactions (STRING) [29]. The network for the initial proteome of 322 proteins consists of 4264 edges. The sub network that spans only OER-derived proteome (73 proteins, 207 pair wise functional associations, Fig. 5) has an average functional association 0.454. This is significantly more than the initial proteome (average functional interaction 0.406, $P<0.01$ Wilcoxon rank sum test). The higher connectivity of the OER-derived proteome provides independent evidence that the enrichment procedure indeed selects for phagosomal

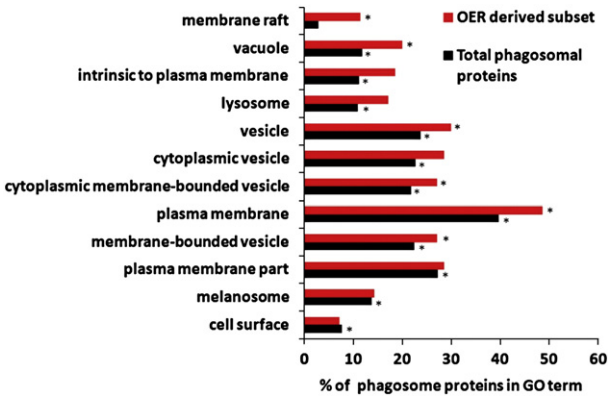

Fig. 4 – Gene Ontology enrichment analysis. Shown are GO terms significantly enriched in the initial set and/or the OER-derived set (*=p-value<0.01). Plotted for each GO term is the percentage of proteins annotated to that term from either the whole phagosome dataset (322 proteins) or OER-derived subset (73 proteins).

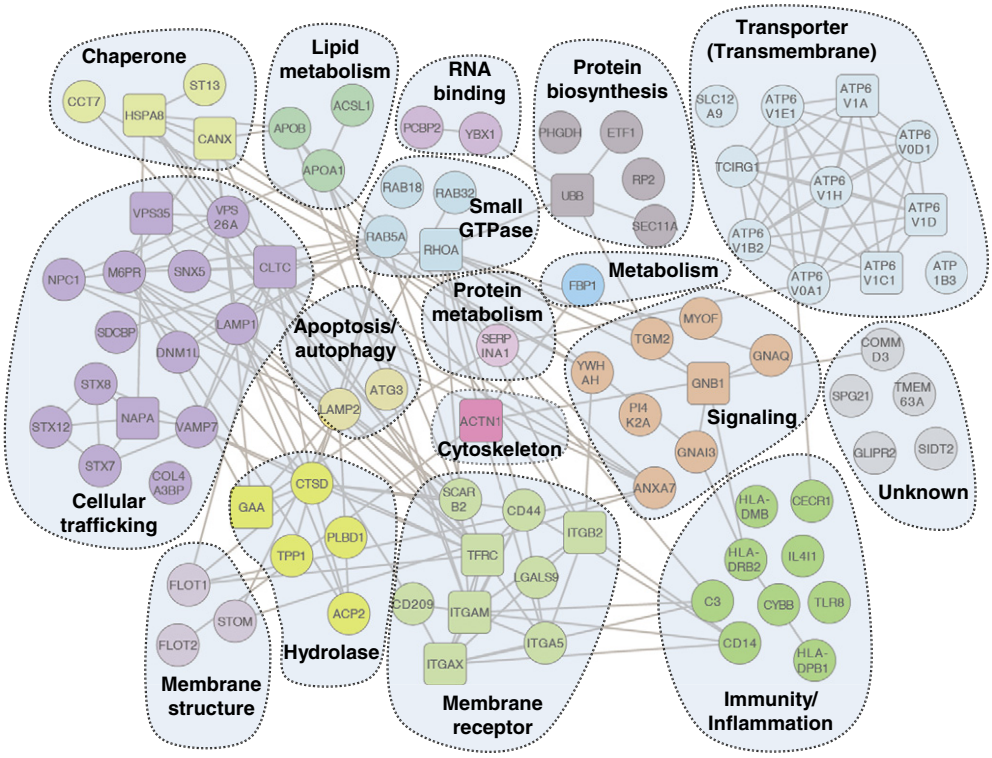

Fig. 5 – Extension of DC phagosome proteome with functionally associated proteins. Shown are functional associations between phagosomal proteins derived from the STRING database [25] (confidence level > 0.5). Round nodes represent phagosomal proteins from the OER-derived subset enriched in phagosomes, rectangles represent additional proteins "rescued" because of high functional association with proteins from the OER-derived subset (association with at least 4 nodes of the OER-derived subset, see Materials and methods for details). Proteins were classified according to Boulais et al [8].

proteins that are robustly functionally related within the cellular compartment.

Encouraged by this result, we decided to extend the OER-derived network with proteins from the initial dataset that did not meet the enrichment threshold. We expect that number of proteins relevant for phagosome function were not included in the OER-derived proteome due to experimental limitations in quantitatively detecting hydrophobic parts of the membrane proteins or because proteins are being expressed and important in multiple cellular compartments, and therefore not enriched specifically in the phagosomal organelle. Using OER alone we cannot identify these proteins but we are able to "rescue" several non-enriched phagosomal proteins using their functional associations to enriched components from our OER-derived dataset. After testing multiple functional association thresholds and topology constraints (see Materials and methods and Supplementary Table 4) we included nodes that are connected to the OER-derived proteome with at least four edges, each at least 0.5 combined score. The network was thus extended (Fig. 5), rescuing 17 proteins from the initial proteome that did not pass the initial enrichment factor threshold. The rescued proteins include, as expected, components of the membrane vacuolar ATPase (completing the set of detected ATPase subunits), four membrane receptors as well as several signaling and trafficking proteins (Fig. 5). This additional procedure extends the phagosome proteome to 90 proteins, improving the detection rate of the positive marker set from 70 to 85%, as well as lowering the cFDR estimate upper limit from 12 to 10% (Supplementary Table 5).

Having composed a phagosome protein set cleaned of many contaminants, we investigated which of these proteins prone to be relevant for DC phagosome function are now specifically identified in DC phagosomes. From the 90 proteins in the extended OER set, 22 were only detected in DC phagosomes and neither in macrophages, THP1 cells nor neutrophils and may thus be specifically important for DC phagosome function (Fig. 6 and Supplementary Table 3). In addition to pattern recognition receptors DC-SIGN and TLR8 these include several plasma protein possibly acquired from the culture medium (such as APOB and SERPINA1), proteins involved in intracellular protein sorting and trafficking (FLOT2, SNX5, DNM1L, ATG3) and several proteins whose function is less well documented, including the lysosomal transmembrane protein SIDT2, ceramide binding COL4A3BP, IL-4 induced L-amino acid oxidase IL4I1 and the adenodisine deaminase CECR1.

3.3. *In vitro validation of OER and identification of Galectin-9 as a phagosomal protein in DCs*

Cleaned up from most co-purified proteins the OER-derived proteome is now much better suited for extracting novel players in (DC) phagocytosis (Fig. 6). To validate our approach and to extrapolate our results to multiple human donors, we

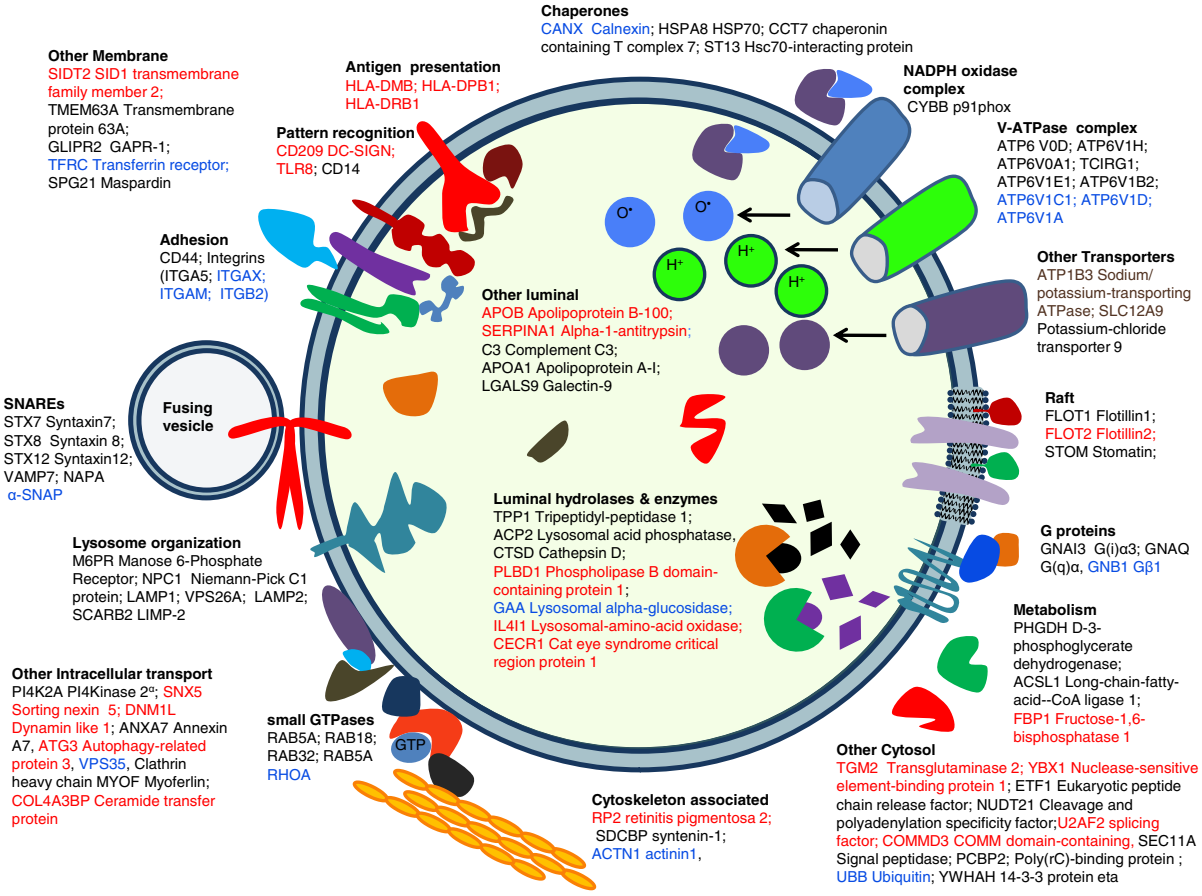

Fig. 6 – Graphical representation of the extended OER derived DC phagosome proteome. Proteins enriched on phagosomes as compared to whole DC are depicted in black, those added to the set by functional association in blue and those uniquely identified in DC phagosomes but not RAW or THP-1 phagosomes, are represented in red.

analyzed isolated phagosomes from 4 pooled donors by Western blotting. We selected a number of known relevant phagosomal constituents from the OER-derived proteome and compared their relative enrichment in phagosomes with respect to post nuclear supernatant (PNS). Note that the Western blot data can only be used for a comparison of enrichment of the proteins with respect to each other as we could not measure the protein concentration of the phagosome sample reliably. Nonetheless, the Western blot confirmed the phagosomal presence and highest enrichment of the high ranking proteins HLA II (DR/DP), DC-SIGN, LAMP1, Cathepsin D (Fig. 7). We also selected several proteins that are depleted from phagosomes according to OER, and indeed found none of these proteins (Actin, Moesin and Cofilin) as enriched by Western blotting. These results are consistent with the importance of the Actin cytoskeleton only at the initial phase of phagocytosis and with the use of Mg-ATP in the isolation procedure to remove/disrupt the actin meshwork.

We also selected Galectin-9 (enrichment factor 1.97) from the OER-derived proteome based on its abundant presence on DC phagosomes, its reported importance in the immune system and its potential interesting implications for DC biology [36,37]. Thus far, Galectin-9 has not been associated with phagocytosis. Consistent with OER, we indeed found Galectin-9 to be recruited to the same extent as DC-SIGN and LAMP1 on isolated DC phagosomes from 4 pooled donors by Western blotting (Fig. 7), indicating its selective incorporation. We detected two isoforms of Galectin-9 with a molecular weight most likely corresponding to the medium and long isoforms (36 and 39 kDA respectively) in both PNS and phagosomes, indicating that these isoforms of Galectin-9 are both recruited to the phagosome.

Although Western blotting can readily demonstrate the relative enrichment of established marker proteins and Galectin-9 in the whole phagosomal preparation, it does not provide quantitative information on individual phagosomes. To quantify this in greater detail, we used flow cytometry that allows analysis of individual phagosomes. This demonstrated that similar to HLA II, LAMP1 and CD44 the majority of phagosomes is positive for Galectin-9 (Fig. 7B). Also within whole cells subjected to confocal microscopy, Galectin-9 was readily seen as a ring around LBC phagosomes (Fig. 8). In addition, Galectin-9 was present throughout the cell but concentrated in the perinuclear area and on membrane ruffles. On phagosomes, Galectin-9 was not only present on

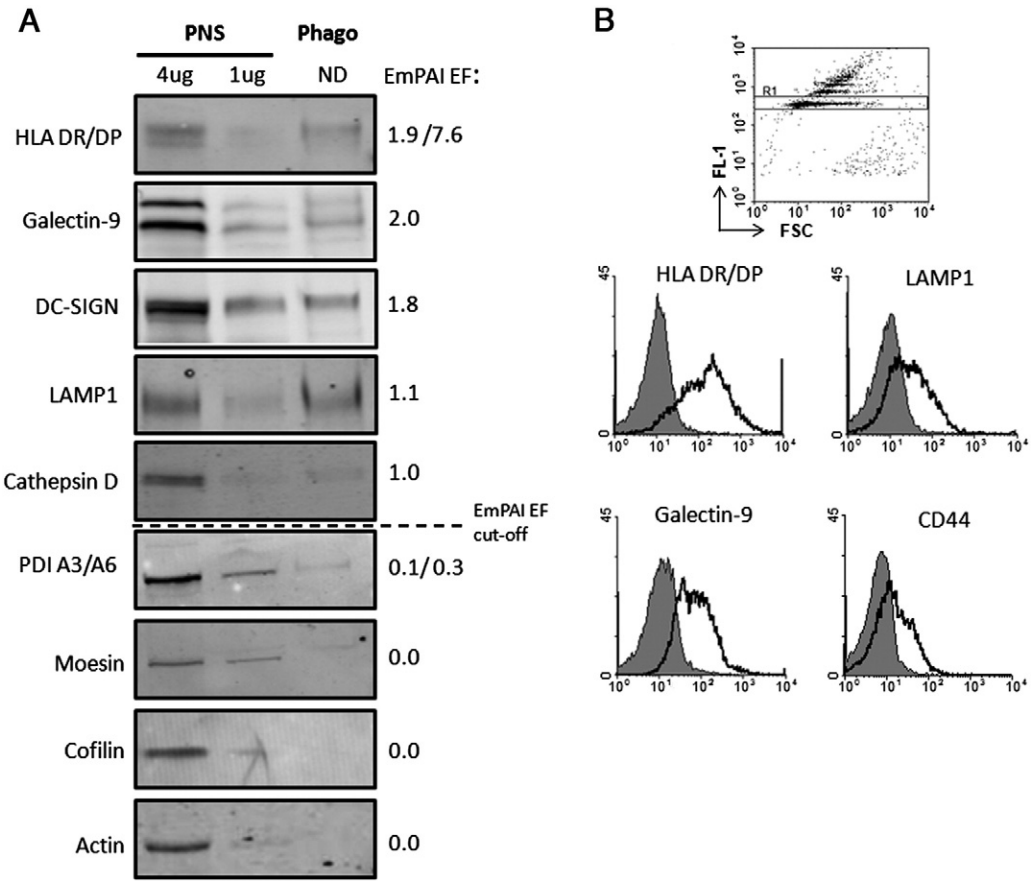

Fig. 7 – In vitro confirmation phagosomal enrichment from 4 pooled donors. A: For the indicated proteins, the Western blot signal of 1 μg and 4 μ g of post nuclear supernatant (PNS) is compared to a sample of isolated phagosomes (of which the protein concentration, due to the antibody coating, could not be determined (ND). All images were obtained from immunolabelings of one single blotting membrane. The presence of the different proteins in phagosomes with respect to PNS can thus be directly compared. Indicated on the right is the emPAI based OER enrichment factor (EF) as determined by MS. In case of HLA and PDI the antibody recognizes more than one protein (e.g. HLA DR and HLA DP) and therefore the OER EF for both proteins is depicted. B: Isolated phagosomes were immunolabeled and analyzed by flow cytometry. Gating of single phagosomes is shown in the upper dot plot (the gate is indicated by R1). Displayed in the lower 3 histograms are phagosomes from R1 labeled with respectively HLA DR/DP, LAMP1 and Galectin-9 antibodies and corresponding isotype control antibodies (grey area).

more mature phagosomes like the ones used for proteomics but was present already early (at 10 min) after the initiation of phagocytosis (Fig. 8A and Supplementary Fig. 3).

Experiments so far had been performed on LBC phagosomes exclusively. Next, we tested whether Galectin-9 was also recruited to pathogen or pathogen extract containing phagosomes. All tested conditions (Zymosan (a *S. cerevisiae* cell wall extract), *C. albicans*, and *S. aureus*) readily recruited Galectin-9 to the enclosing phagosome membrane, suggesting that Galectin-9 recruitment is functionally important in DC-phagosomes irrespective of cargo that is phagocytosed (Fig. 8B). Finally we investigated the possible origin of phagosomal galectin-9. Galectins are known to be present as soluble proteins in the cytosol or to be secreted after which they can bind to sugar modified cell surface receptors or may even be present as transmembrane proteins [36]. Indeed on iDC Galectin-9 could be readily detected bound to the cell surface (Fig. 8C). In addition a large pool of Galectin-9 could only be reached after permeabilisation and thus resides intracellular (Fig. 8B). CD44, a known binding partner of Galectin-9 [38,39] and a phagocytic receptor [40] was also present in the OER derived subset and detected on DC phagosomes (Figs. 5, 6 and 7), opening up the possibility that Galectin-9 was incorporated into phagosomes via it's interaction with CD44. Although this topic requires further investigation, already in favor of this hypothesis we found that CD44 and Galectin-9 showed marked co-localization on the DC surface upon antibody induced crosslinking (Pearson correlation coefficient 0.76± 0.14) suggesting close proximity of the two proteins.

4. Discussion

Here, we present the first comprehensive proteome analysis of phagosomes derived from human DCs. Moreover, we used a subtractive approach (OER), comparing protein abundance in isolated phagosomes to whole cells to effectively select proteins prone to be relevant for phagosome function or biogenesis, from the large set of proteins identified on isolated phagosomes. In this way we facilitate the translation of

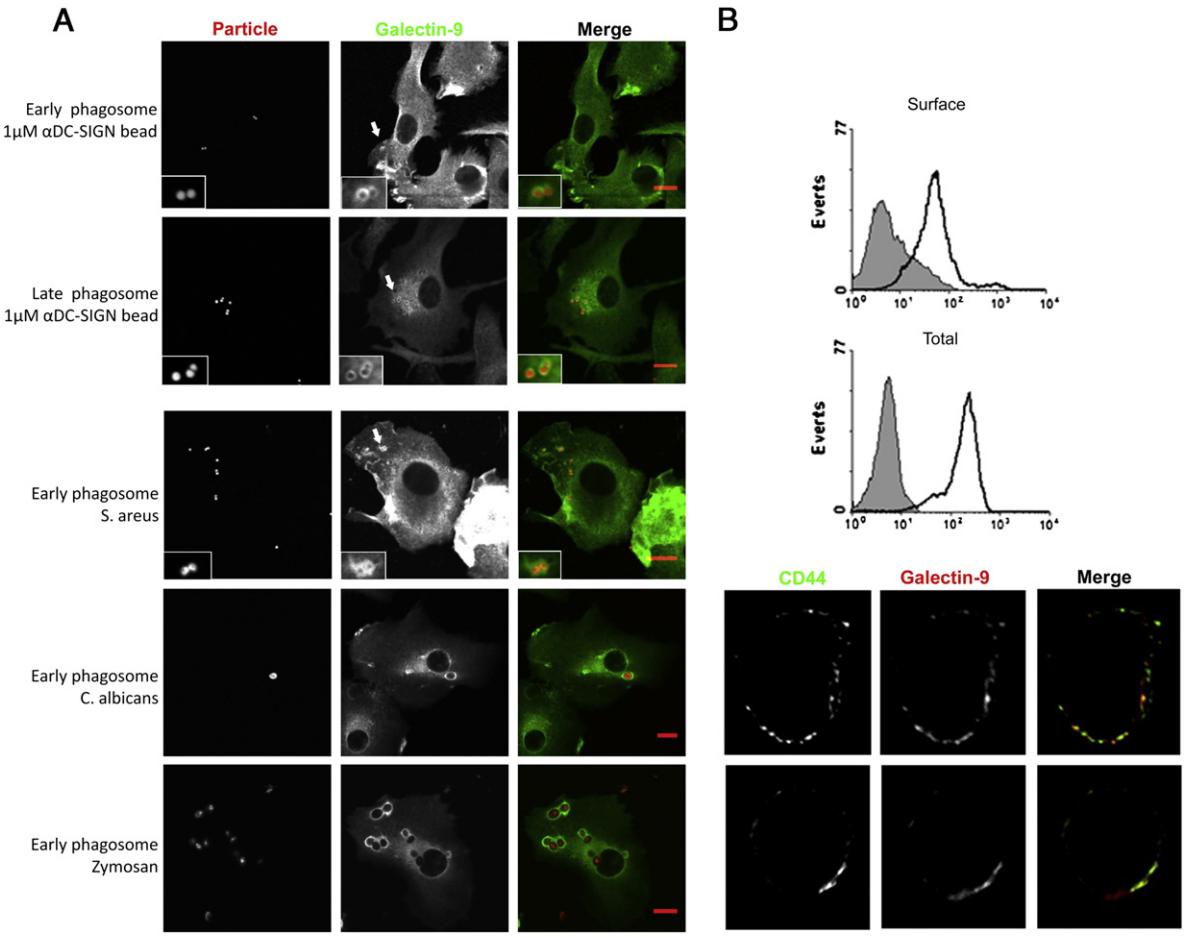

Fig. 8 – Galectin-9 recruitment in DC phagocytosis. A: DCs were incubated with 1 μm fluorescent anti-DC-SIGN coated beads for 10 min (early phagosomes) and for 1 h, followed by a 1 h chase (late phagosomes). B: DCs were incubated with fluorescently labeled pathogen derived particulates (*S. areus*, *C. albicans*, and Zymosan) for 10 min (early phagosomes). Cells were subsequently immunolabeled for Galectin-9 and analyzed by confocal microscopy. On each row fluorescence of the particles is visible in the left panel, Galectin-9 staining in the middle panel and the colored overlay of both signals is visible in the right panel. Insets depict magnifications of the areas indicated by the white arrow. Bar 10 μm. C: Immature DC were fixed and immunolabeled for Galectin-9 in the absence (surface Galectin-9) or presence of detergent (total Galectin-9) Isotype control standings are depicted by the grey filled histograms. D: live Immature DC were labeled for both CD44 and Galectin-9 on ice and subsequently crosslinked at 15° by fluorescently conjugated secondary antibodies. Shown signals for CD44 (left panel), Galectin-9 (middle panel) and the colored overlay (right panels) for two representative cells.

organellar proteomics data into biological function. Thus the OER-derived phagosome proteome can now be used as a more efficient starting point for the identification of novel phagosomal proteins important for (DC) phagocytosis.

With the sensitivity of current MS analysis hundreds proteins are discovered in phagosome preparations or other subcellular isolates that not only include proteins relevant for organelle function but also traces of co-purified proteins. These proteins significantly complicate biological interpretation and hamper selection of proteins for additional functional studies. This has been recognized by other researcher and several strategies to overcome this problem have been developed including PCP [11] (protein correlation profiling of the purified organelle to earlier steps in the purification procedure), LOPIT [41] (localization of organelle proteins by isotope tagging), and specifically for phagosomes, restriction to proteins that are dynamically associated to phagosomes in time or after a specific stimulus [10,28]. The use of such elaborate, material demanding methods however is not always feasible especially not when studying primary cells such as DCs, which can only be obtained in limited numbers. Therefore phagosomal proteomes of primary cells are generally derived directly from purifications of phagosomes, where only sample purity critically dictates the quality of the proteome. Here we exploited a label free strategy to “clean up” and bring focus to the organellar proteome, by quantitatively comparing organellar protein abundance with protein abundance in a previously measured representative of the cell of origin (in this case the dendritic cell). Although others have compared different isolated subcellular fractions with each other before to determine whether a protein is a bona fide constituent of a purified organelle [11–14] this is to the best of our knowledge the first

time a subtractive method has been tested to determine the phagosome proteome where the whole cell of origin was used as a reference.

The validity of the OER method was verified for several proteins by Western blotting, where an analogous enrichment analysis of purified organelle versus starting material has been common practice for a long period of time. Obviously, the best result can be expected from closely matching reference sets, but we could demonstrate that even when a non-identical (e.g. from another donor) and not simultaneously prepared or measured reference set of DC was used, significant "cleaning" of proteome data was observed. This implicates that one may also use background datasets of label-free quantified whole cell proteomes generated by others to perform OER, an important finding in an era taking increasing advantage of web-based data sharing.

From an initial phagosome proteome of 322 proteins, we present an OER-derived core set of 73 phagosomal DC proteins, further extended by functional interaction to 90 proteins, which contains less than 10% passively co-purified proteins. We thus have defined a pure high-quality phagosome proteome that we can now use as a more efficient starting point for further investigation. This proteome contains 22 proteins uniquely associated to the DC phagosome that may have implications for DC specific phagosome functions. In addition the extended OER-derived proteome contains many proteins previously associated with phagosomes from other cell types, such as proteins involved in intracellular membrane and proteins trafficking (e.g. SNARE proteins, Rab GTPases, Flotillins, PRR and adhesion molecules [7]. Not all these proteins could be *a priori* included in our positive marker set, because phagosomal association of these proteins has been confirmed in other cell types than DCs or because they do not necessarily associate with the phagosome at this time-point. The phagosome proteome is highly dynamic, with many proteins recruited to the phagosome that are also removed again with time (e.g. MHC I and components of its loading machinery, Rab GTPases, cytoskeleton). This results in a variation of phagosomal abundances that is related to phagosome age [10,42]. Relative abundance may thus also reflect the extent to which a protein is important in a particular phase of phagosome maturation. For such proteins, exclusion from our OER-derived proteome, implicates merely that they are not as relevant for the phagosome at this stage (e.g. the phago-lysosome) but it does not mean they are not relevant at an earlier or later time point of phagocytosis. Furthermore, the organellar enrichment analysis may discard proteins that are also abundantly expressed in other cellular compartments such as the cytoskeleton or ER and are therefore not enriched on the phagosome. These proteins may still have an important function in the phagosome. This drawback however, not only applies to OER but also to PCP or to more conventional techniques such as Western blotting. We have attempted to overcome this issue by analyzing the functional association between the OER-derived and the initial proteome, rescuing proteins that are functionally highly related to the OER-derived core set. Indeed, using functional association we further extended our OER proteome to a final set of 90 proteins and also further improved the sensitivity and FDR of our approach to 85% and less than 10% respectively. Although functional association allows us to rescue several non-enriched proteins the design of our method will mean that we will inevitably discard as small fraction (15%) of phagosomal proteins with a broad cellular distribution and function. The importance of these proteins for phagosome biology must therefore be revealed using other strategies.

Recently there has been much debate on the involvement of the ER in phagosome biogenesis and it has been held responsible for the crosspresenting abilities of this compartment in DC [43–45]. Consistent with previous results obtained by Touret, Rogers et al. [10,46] our results do not indicate a major contribution of ER proteins on to the DC phagosome proteome at the time-point that was the focus of our study. Nevertheless, our data do indicate that ER components dedicated to the peptide loading of MHC I are overrepresented in protein counts on DC phagosomes compared to whole DC. These proteins however were not found to be enriched in terms of abundance, which could either be a result of the high overall cellular presence of these proteins or the result of a diminishing HLA I loading capacity in the more mature phagosome. Although this topic demands additional experimental evidence, the selective presence of the MHC I loading machinery over total ER may indicate that only a subset of ER proteins is transferred to or remains on the DC phagosome, a distinction that cannot be made based solely on the present data.

Many of the constituents of the final extended OER-derived proteome represent proteins involved in phagosomal dynamics regulating the fusion with other (endocytic) organelles (including Rab GTPases, SNARE proteins, LAMPs, Annexins and lipid modulating enzymes) or enzymes responsible for lysosomal hydrolysis of proteins, sugars and lipids. Regulating the quantity and type of antigenic epitopes generated, these hydrolases have potential implications for DC protein and lipid antigen presentation [2]. Also, several transmembrane receptors with known function in DCs are present in the core proteome including the phagocytic/adhesive αMβ2-integrin [47], CD44 [48] and α5-integrin subunit [49], the immune suppressive receptor LILRB2 [50] and finally the pattern recognition receptors TLR8 [34] and CD14 [51]. Intriguingly, CD14 is downregulated during DC differentiation from monocytes and therefore hardly present on (the surface of) immature DC [52]. On monocytes CD14 mainly functions as a co-receptor for extracellular TLR4 that detects bacterial lipopolysaccharides. Its presence in DC phagosomes could indicate that in DCs a small amount of CD14 may remain to aid signaling from other intracellular TLR, as has been recently reported [53]. A candidate for CD14 regulation would be TLR8 that we have also identified on phagosomes here.

In addition, several other transmembrane proteins are identified that may have implications for DC immune function such as TMEM63A with a yet unknown function, the recently described lysosomal protein SIDT2 [54] and GLIPR2 (GAPR1) [55]. GAPR1 is predominantly expressed within the immune system further supporting its role in immunity.

Also, the electrolyte balance in phagosomes is of crucial importance for antigen processing and presentation. Besides components of the V-ATPase complex and the NADPH-oxidase complex (Nox2), regulating the pH [35], other

transporters were indentified in the enriched subset as well, including the poorly studied Na^+/K^+ transporter ATP1B3 expressed on all blood leukocytes [56] and SLC12A9, with unknown shuttling substrate [57] that may exert their effect on DC phagosome function by shuttling ions or small molecules over the phagosomal membrane.

Intriguingly, we identified Galectin-9 as a novel protein recruited to the phagosome of DCs. Galectin-9 is a β-galactoside binding lectin composed of two different carbohydrate recognition domains (CRD) connected by a linker molecule [36]. Several studies show that Galectin-9 is involved in adhesion, acts as an eosinophil chemo-attractant, triggers signaling in ostoblasts, possibly induces maturation in dendritic cells, regulates thymocyte–endothelial interactions and seems implicated in triggering apoptosis in thymocytes [39,58–62]. Interestingly, Galectin-9 was found to interact with CD44 and modulates its signaling and adhesive properties [38,39]. We classified CD44 as enriched in DC phagosomes by OER, confirmed its presence on isolated phagosomes by flow cytometry and intriguingly showed Galectin-9 and CD44 are in close proximity at the DC plasma membrane. It is therefore tempting to speculate that these proteins also act in concert here [38,63].

In relation to its functions in the immune system, Galectin-9 has mainly been described as cytosolic, secreted or attached to the plasma membrane via its carbohydrate recognition domains. Intriguingly, Galectin-9 has also been shown to be identical to the urate transporter UAT1 that was found to exist as a transmembrane protein with its CRD domains on the extracellular side [64]. Therefore, Galectin-9 associates to the phagosome on either the luminal or cytosolic side, or alternatively transverses the phagosome membrane. Although it's presence on the cell surface and its proximity to CD44 suggest Galectin-9 may be incorporated in phagosomes trough associated with CD44 or with other glycosylated cell surface proteins it cannot be excluded that phagosomal Galectin-9 even has channel like properties regulated by its CRD domains [64].

5. Conclusion

In conclusion, here we present the first proteome of human DC phagosomes defined by OER in conjunction with functional association that can now effectively be used to identify novel players on (DC) phagosomes. We demonstrate that the use of a reference cell for the analysis of organellar proteomes is an efficient way to discriminate true organellar constituents from co-purified proteins. We show that OER can even be performed with a non-identical reference set, which makes it a general method that opens up the use of reference sets available in the public domain for this method. We believe that – with the growing sensitivity of state-of-the art mass spectrometry in the sub femtomol range – a general procedure like enrichment ranking that eliminates co-purified proteins from purified organelles is an essential step for the translation of large scale organellar proteome data to biological function.

Supplementary materials related to this article can be found online at doi:10.1016/j.jprot.2011.11.024.

Acknowledgments

The authors would like to thank the Nijmegen Proteomics Facility for usage of the MS instrumentation. R.S. was supported by Horizon grant (050-71-053) from the Netherlands Organization for Scientific Research (NWO). This work was supported by the Netherlands Organization for Scientific Research (NWO) grant, number 9120.6030.

REFERENCES

[1] Banchereau J, Steinman RM. Dendritic cells and the control of immunity. Nature 1998;392:245–52.
[2] Savina A, Amigorena S. Phagocytosis and antigen presentation in dendritic cells. Immunol Rev 2007;219:143–56.
[3] Stuart LM, Ezekowitz RA. Phagocytosis: elegant complexity. Immunity 2005;22:539–50.
[4] Blander JM. Signalling and phagocytosis in the orchestration of host defence. Cell Microbiol 2007;9:290–9.
[5] Underhill DM, Gantner B. Integration of Toll-like receptor and phagocytic signaling for tailored immunity. Microbes Infect 2004;6:1368–73.
[6] Rogers LD, Foster LJ. Contributions of proteomics to understanding phagosome maturation. Cell Microbiol 2008;10:1405–12.
[7] Li Q, Jagannath C, Rao PK, Singh CR, Lostumbo G. Analysis of phagosomal proteomes: from latex-bead to bacterial phagosomes. Proteomics 2010;10:4098–116.
[8] Boulais J, Trost M, Landry CR, Dieckmann R, Levy ED, Soldati T, et al. Molecular characterization of the evolution of phagosomes. Mol Syst Biol 2010;6:423.
[9] Ishihama Y, Oda Y, Tabata T, Sato T, Nagasu T, Rappsilber J, et al. Exponentially modified protein abundance index (emPAI) for estimation of absolute protein amount in proteomics by the number of sequenced peptides per protein. Mol Cell Proteomics 2005;4:1265–72.
[10] Rogers LD, Foster LJ. The dynamic phagosomal proteome and the contribution of the endoplasmic reticulum. Proc Natl Acad Sci U S A 2007;104:18520–5.
[11] Foster LJ, de Hoog CL, Zhang Y, Zhang Y, Xie X, Mootha VK, et al. A mammalian organelle map by protein correlation profiling. Cell 2006;125:187–99.
[12] Borner GH, Harbour M, Hester S, Lilley KS, Robinson MS. Comparative proteomics of clathrin-coated vesicles. J Cell Biol 2006;175:571–8.
[13] Zheng YZ, Berg KB, Foster LJ. Mitochondria do not contain lipid rafts, and lipid rafts do not contain mitochondrial proteins. J Lipid Res 2009;50:988–98.
[14] Gilchrist A, Au CE, Hiding J, Bell AW, Fernandez-Rodriguez J, Lesimple S, et al. Quantitative proteomics analysis of the secretory pathway. Cell 2006;127:1265–81.
[15] Jonuleit H, Kuhn U, Muller G, Steinbrink K, Paragnik L, Schmitt E, et al. Pro-inflammatory cytokines and prostaglandins induce maturation of potent immunostimulatory dendritic cells under fetal calf serum-free conditions. Eur J Immunol 1997;27:3135–42.
[16] Desjardins M, Celis JE, van Meer G, Dieplinger H, Jahraus A, Griffiths G, et al. Molecular characterization of phagosomes. J Biol Chem 1994;269:32194–200.
[17] Bolte S, Cordelieres FP. A guided tour into subcellular colocalization analysis in light microscopy. J Microsc 2006;224:213–32.
[18] Tacken PJ, de Vries IJ, Gijzen K, Joosten B, Wu D, Rother RP, et al. Effective induction of naive and recall T-cell responses

by targeting antigen to human dendritic cells via a humanized anti-DC-SIGN antibody. Blood 2005;106:1278–85.
[19] Lasonder E, Ishihama Y, Andersen JS, Vermunt AM, Pain A, Sauerwein RW, et al. Analysis of the *Plasmodium falciparum* proteome by high-accuracy mass spectrometry. Nature 2002;419:537–42.
[20] Rappsilber J, Ishihama Y, Mann M. Stop and go extraction tips for matrix-assisted laser desorption/ionization, nanoelectrospray, and LC/MS sample pretreatment in proteomics. Anal Chem 2003;75:663–70.
[21] Cox J, Mann M. MaxQuant enables high peptide identification rates, individualized p.p.b.-range mass accuracies and proteome-wide protein quantification. Nat Biotechnol 2008;26:1367–72.
[22] Ishihama Y, Schmidt T, Rappsilber J, Mann M, Hartl FU, Kerner MJ, et al. Protein abundance profiling of the *Escherichia coli* cytosol. BMC Genomics 2008;9:102.
[23] Buschow SI, Lasonder E, van Deutekom HW, Oud MM, Beltrame L, Huynen MA, et al. Dominant processes during human dendritic cell maturation revealed by integration of proteome and transcriptome at the pathway level. J Proteome Res 2010;9:1727–37.
[24] Dennis Jr G, Sherman BT, Hosack DA, Yang J, Gao W, Lane HC, et al. DAVID: Database for Annotation, Visualization, and Integrated Discovery. Genome Biol 2003;4:P3.
[25] Hosack DA, Dennis Jr G, Sherman BT, Lane HC, Lempicki RA. Identifying biological themes within lists of genes with EASE. Genome Biol 2003;4:R70.
[26] Burlak C, Whitney AR, Mead DJ, Hackstadt T, Deleo FR. Maturation of human neutrophil phagosomes includes incorporation of molecular chaperones and endoplasmic reticulum quality control machinery. Mol Cell Proteomics 2006;5:620–34.
[27] Lee BY, Jethwaney D, Schilling B, Clemens DL, Gibson BW, Horwitz MA. The *Mycobacterium bovis* bacille Calmette-Guerin phagosome proteome. Mol Cell Proteomics 2010;9:32–53.
[28] Trost M, English L, Lemieux S, Courcelles M, Desjardins M, Thibault P. The phagosomal proteome in interferon-gamma-activated macrophages. Immunity 2009;30:143–54.
[29] Szklarczyk D, Franceschini A, Kuhn M, Simonovic M, Roth A, Minguez P, et al. The STRING database in 2011: functional interaction networks of proteins, globally integrated and scored. Nucleic Acids Res 2011;39:D561–8.
[30] Engering A, Geijtenbeek TB, van Vliet SJ, Wijers M, van Liempt E, Demaurex N, et al. The dendritic cell-specific adhesion receptor DC-SIGN internalizes antigen for presentation to T cells. J Immunol 2002;168:2118–26.
[31] Cambi A, Gijzen K, de Vries JM, Torensma R, Joosten B, Adema GJ, et al. The C-type lectin DC-SIGN (CD209) is an antigen-uptake receptor for *Candida albicans* on dendritic cells. Eur J Immunol 2003;33:532–8.
[32] Gringhuis SI, den Dunnen J, Litjens M, van der Vlist M, Geijtenbeek TB. Carbohydrate-specific signaling through the DC-SIGN signalosome tailors immunity to Mycobacterium tuberculosis, HIV-1 and Helicobacter pylori. Nat Immunol 2009;10:1081–8.
[33] Gringhuis SI, den Dunnen J, Litjens M, van Het Hof B, van Kooyk Y, Geijtenbeek TB. C-type lectin DC-SIGN modulates Toll-like receptor signaling via Raf-1 kinase-dependent acetylation of transcription factor NF-kappaB. Immunity 2007;26:605–16.
[34] Heil F, Hemmi H, Hochrein H, Ampenberger F, Kirschning C, Akira S, et al. Species-specific recognition of single-stranded RNA via toll-like receptor 7 and 8. Science 2004;303:1526–9.
[35] Mantegazza AR, Savina A, Vermeulen M, Perez L, Geffner J, Hermine O, et al. NADPH oxidase controls phagosomal pH and antigen cross-presentation in human dendritic cells. Blood 2008;112:4712–22.
[36] Rabinovich GA, Toscano MA. Turning 'sweet' on immunity: galectin–glycan interactions in immune tolerance and inflammation. Nat Rev 2009;9:338–52.
[37] Sato S, St-Pierre C, Bhaumik P, Nieminen J. Galectins in innate immunity: dual functions of host soluble beta-galactoside-binding lectins as damage-associated molecular patterns (DAMPs) and as receptors for pathogen-associated molecular patterns (PAMPs). Immunol Rev 2009;230:172–87.
[38] Katoh S, Ishii N, Nobumoto A, Takeshita K, Dai SY, Shinonaga R, et al. Galectin-9 inhibits CD44-hyaluronan interaction and suppresses a murine model of allergic asthma. Am J Respir Crit Care Med 2007;176:27–35.
[39] Tanikawa R, Tanikawa T, Hirashima M, Yamauchi A, Tanaka Y. Galectin-9 induces osteoblast differentiation through the CD44/Smad signaling pathway. Biochem Biophys Res Commun 2010;394:317–22.
[40] Vachon E, Martin R, Plumb J, Kwok V, Vandivier RW, Glogauer M, et al. CD44 is a phagocytic receptor. Blood 2006;107: 4149–58.
[41] Dunkley TP, Watson R, Griffin JL, Dupree P, Lilley KS. Localization of organelle proteins by isotope tagging (LOPIT). Mol Cell Proteomics 2004;3:1128–34.
[42] Haas A. The phagosome: compartment with a license to kill. Traffic 2007;8:311–30.
[43] Gagnon E, Duclos S, Rondeau C, Chevet E, Cameron PH, Steele-Mortimer O, et al. Endoplasmic reticulum-mediated phagocytosis is a mechanism of entry into macrophages. Cell 2002;110:119–31.
[44] Guermonprez P, Saveanu L, Kleijmeer M, Davoust J, Van Endert P, Amigorena S. ER-phagosome fusion defines an MHC class I cross-presentation compartment in dendritic cells. Nature 2003;425:397–402.
[45] Ackerman AL, Giodini A, Cresswell P. A role for the endoplasmic reticulum protein retrotranslocation machinery during crosspresentation by dendritic cells. Immunity 2006;25:607–17.
[46] Touret N, Paroutis P, Terebiznik M, Harrison RE, Trombetta S, Pypaert M, et al. Quantitative and dynamic assessment of the contribution of the ER to phagosome formation. Cell 2005;123: 157–70.
[47] Ehlers MR. CR3: a general purpose adhesion-recognition receptor essential for innate immunity. Microbes Infect 2000;2:289–94.
[48] Vachon E, Martin R, Kwok V, Cherepanov V, Chow CW, Doerschuk CM, et al. CD44-mediated phagocytosis induces inside-out activation of complement receptor-3 in murine macrophages. Blood 2007;110:4492–502.
[49] van Helden SF, Krooshoop DJ, Broers KC, Raymakers RA, Figdor CG, van Leeuwen FN. A critical role for prostaglandin E2 in podosome dissolution and induction of high-speed migration during dendritic cell maturation. J Immunol 2006;177:1567–74.
[50] Brown DP, Jones DC, Anderson KJ, Lapaque N, Buerki RA, Trowsdale J, et al. The inhibitory receptor LILRB4 (ILT3) modulates antigen presenting cell phenotype and, along with LILRB2 (ILT4), is upregulated in response to Salmonella infection. BMC Immunol 2009;10:56.
[51] Akashi-Takamura S, Miyake K. TLR accessory molecules. Curr Opin Immunol 2008;20:420–5.
[52] Chapuis F, Rosenzwajg M, Yagello M, Ekman M, Biberfeld P, Gluckman JC. Differentiation of human dendritic cells from monocytes in vitro. Eur J Immunol 1997;27:431–41.
[53] Baumann CL, Aspalter IM, Sharif O, Pichlmair A, Bluml S, Grebien F, et al. CD14 is a coreceptor of Toll-like receptors 7 and 9. J Exp Med 2010;207:2689–701.
[54] Jialin G, Xuefan G, Huiwen Z. SID1 transmembrane family, member 2 (Sidt2): a novel lysosomal membrane protein. Biochem Biophys Res Commun 2010;402:588–94.

[55] Eberle HB, Serrano RL, Fullekrug J, Schlosser A, Lehmann WD, Lottspeich F, et al. Identification and characterization of a novel human plant pathogenesis-related protein that localizes to lipid-enriched microdomains in the Golgi complex. J Cell Sci 2002;115:827–38.
[56] Chiampanichayakul S, Khunkaewla P, Pata S, Kasinrerk W. Na, K ATPase beta3 subunit (CD298): association with alpha subunit and expression on peripheral blood cells. Tissue Antigens 2006;68:509–17.
[57] Hebert SC, Mount DB, Gamba G. Molecular physiology of cation-coupled Cl– cotransport: the SLC12 family. Pflugers Arch 2004;447:580–93.
[58] Matsumoto R, Matsumoto H, Seki M, Hata M, Asano Y, Kanegasaki S, et al. Human ecalectin, a variant of human galectin-9, is a novel eosinophil chemoattractant produced by T lymphocytes. J Biol Chem 1998;273:16976–84.
[59] Dai SY, Nakagawa R, Itoh A, Murakami H, Kashio Y, Abe H, et al. Galectin-9 induces maturation of human monocyte-derived dendritic cells. J Immunol 2005;175:2974–81.
[60] Tanikawa R, Tanikawa T, Okada Y, Nakano K, Hirashima M, Yamauchi A, et al. Interaction of galectin-9 with lipid rafts induces osteoblast proliferation through the c-Src/ERK signaling pathway. J Bone Miner Res 2008;23:278–86.
[61] Wada J, Ota K, Kumar A, Wallner EI, Kanwar YS. Developmental regulation, expression, and apoptotic potential of galectin-9, a beta-galactoside binding lectin. J Clin Invest 1997;99:2452–61.
[62] Nobumoto A, Nagahara K, Oomizu S, Katoh S, Nishi N, Takeshita K, et al. Galectin-9 suppresses tumor metastasis by blocking adhesion to endothelium and extracellular matrices. Glycobiology 2008;18:735–44.
[63] Tanikawa R, Tanikawa T, Hirashima M, Yamauchi A, Tanaka Y. Galectin-9 induces osteoblast differentiation through the CD44/Smad signaling pathway. Biochem Biophys Res Commun 2010;394:317–22.
[64] Lipkowitz MS, Leal-Pinto E, Cohen BE, Abramson RG. Galectin 9 is the sugar-regulated urate transporter/channel UAT. Glycoconj J 2004;19:491–8.